XMM-Newton and Swift spectroscopy of the newly discovered very faint X-ray transient IGR J17494-3030

Armas Padilla, M.; Wijnands, R.; Degenaar, N.

Published in:
Monthly Notices of the Royal Astronomical Society. Letters

DOI:
10.1093/mnrasl/slt119

Monthly Notices of the ROYAL ASTRONOMICAL SOCIETY

MNRASL **436,** L89–L93 (2013) doi:10.1093/mnrasl/slt119
Advance Access publication 2013 September 13

XMM–Newton and *Swift* spectroscopy of the newly discovered very faint X-ray transient IGR J17494–3030

M. Armas Padilla,[1]★ R. Wijnands[1] and N. Degenaar[2]†

[1] *Astronomical Institute 'Anton Pannekoek', University of Amsterdam, Postbus 94249, NL-1090 GE Amsterdam, the Netherlands*
[2] *Department of Astronomy, University of Michigan, 500 Church Street, Ann Arbor, MI 48109, USA*

Accepted 2013 August 14. Received 2013 July 29; in original form 2013 July 4

ABSTRACT

A growing group of low-mass X-ray binaries are found to be accreting at very faint X-ray luminosities of $<10^{36}$ erg s^{-1} (2–10 keV). One such system is the new X-ray transient IGR J17494–3030. We present *Swift* and *XMM–Newton* observations obtained during its 2012 discovery outburst. The *Swift* observations trace the peak of the outburst, which reached a luminosity of $\sim 7 \times 10^{35}$ $(D/8\ \mathrm{kpc})^2$ erg s^{-1} (2–10 keV). The *XMM–Newton* data were obtained when the outburst had decayed to an intensity of $\sim 8 \times 10^{34}$ $(D/8\ \mathrm{kpc})^2$ erg s^{-1}. The spectrum can be described by a power law with an index of $\Gamma \sim 1.7$ and requires an additional soft component with a blackbody temperature of ∼0.37 keV (contributing ∼20 per cent to the total unabsorbed flux in the 0.5–10 keV band). Given the similarities with high-quality spectra of very faint neutron-star low-mass X-ray binaries, we suggest that the compact primary in IGR J17494–3030 is a neutron star. Interestingly, the source intensity decreased rapidly during the ∼12 h *XMM–Newton* observation, which was accompanied by a decrease in inferred temperature. We interpret the soft spectral component as arising from the neutron-star surface due to low-level accretion, and propose that the observed decline in intensity was the result of a decrease in the mass-accretion rate on to the neutron star.

Key words: accretion, accretion discs – stars: individual: IGR J17494–3030.

1 INTRODUCTION

Low-mass X-ray binaries (LMXBs) are composed of a black hole or a neutron star that accretes material from a (sub)solar companion star that overflows its Roche lobe. A large fraction of LMXBs remain in a dim quiescence state, during which no or very little accretion occurs and the X-ray luminosity (L_X) is $\sim 10^{30-33}$ erg s^{-1}. However, once in a while, the sources experience outburst events in which their accretion rate increases drastically and consequently their X-ray brightness as well. LMXBs can be classified depending on the maximum 2–10 keV luminosity (L_X^{peak}) that they reach. Those systems that can obtain L_X^{peak} of $\sim 10^{37-39}$ erg s^{-1} are called *(very)bright* systems. The *faint* ones can reach $L_X^{\mathrm{peak}} \sim 10^{36-37}$ erg s^{-1}, and the sources that display L_X^{peak} of only $\sim 10^{34-36}$ erg s^{-1} are called *very faint* X-ray binaries (VFXBs; Wijnands et al. 2006). Despite significant progress over the last few years in our understanding of the behaviour of those VFXBs (Muno et al. 2005; Campana 2009; Degenaar & Wijnands 2009, 2010; Armas Padilla et al. 2011, 2013a; Armas Padilla, Degenaar & Wijnands 2013b), much remains unclear about them (e.g. the mechanism behind their low luminosities is not understood).

One recently discovered VFXB is IGR J17494–3030. The source was first detected during the Galactic Centre *INTEGRAL* observation performed on 2012 March 17–19 (Boissay et al. 2012). Multiple *Swift* X-ray telescope (XRT) observations were obtained (Bozzo et al. 2012) but ∼27 d after the source was first detected, it could not be detected anymore using *Chandra* (Chakrabarty, Jonker & Markwardt 2013). Inspecting the near-infrared (NIR) images acquired on 2010 July as part of the NIR VVV survey (Minniti et al. 2010), five sources could be identified within the *Swift*/XRT error circle. Those sources are potential candidates for the quiescent NIR counterpart of IGR J17494–3030 although it cannot be excluded that none of those sources is associated with the source. In this Letter, we present the analysis of four *Swift* observations and our *XMM–Newton* observation of IGR J17494–3030 obtained during the outburst decay phase.

2 OBSERVATIONS AND REDUCTION

2.1 *XMM–Newton* data

IGR J17494–3030 was observed with *XMM–Newton* (Jansen et al. 2001) on 2012 March 31 for ∼43 ks (see Table 1). The European

★ E-mail: m.armaspadilla@uva.nl
† Hubble fellow.

Table 1. *Swift* and *XMM–Newton* observation log.

Satellite/Instrument	Mode	Observation ID	Date (yyyy-mm-dd)	Exposure time (ks)	Count rate (counts s^{-1})	Net count rate[a] (counts s^{-1})
Swift/XRT	PC	00032318001	2012-03-20	1.0	0.93	0.35
Swift/XRT	WT	00032318002	2012-03-23	1.0	1.89	1.63
Swift/XRT	PC	00032318003	2012-03-26	0.6	0.80	0.39
Swift/XRT	PC	00032318004	2012-03-30	1.1	0.28	0.28
XMM–Newton/EPIC		0694040201	2012-03-31	43.9		
(MOS1)	Imaging				0.44	0.38
(MOS2)	Imaging				0.44	0.38
(PN)	Timing				1.34	0.98

[a]Count rate after background correction, using the annulus regions to mitigate the pile-up in *Swift* obs 00032318001 and 00032318003, and after excluding a short episode of background flaring observed during the *XMM–Newton* observation.

Photon Imaging Camera (EPIC) on board *XMM–Newton* consists of two MOS cameras (Turner et al. 2001) and one PN camera (Strüder et al. 2001). They were operated in imaging (full-frame window) and timing mode, respectively. We reduced the data and obtained scientific products using the Science Analysis Software (SAS, v. 13.0).

We filtered out an episode of background flaring by only selecting data for which the high-energy count rate was $<$0.25 counts s^{-1} ($>$10 keV) for the MOS cameras and $<$0.2 counts s^{-1} (10–12 keV) for the PN. The total resulting live time is ∼42 ks for the MOS cameras and ∼39 ks for the PN detector. For the MOS cameras, we extracted the source event file using a circular region centred on the source position and with a radius of ∼47 arcsec; the background was extracted using a circular region with a radius of ∼107 arcsec centred on a source-free region. The MOS source count rate (Table 1) is below the 0.7 counts s^{-1} pile-up threshold.[1] After correcting the PN data for the transfer inefficiency that affects data obtained using the timing modes,[2] we extracted the source and background events by selecting the data with RAWX columns [32:42] and [5:12], respectively. The PN source count rate (Table 1) is much lower that the pile-up limit of 800 counts s^{-1} for the PN timing mode[1]. We generated the spectra and the light curves as well as the response files applying the standard analysis threads. We grouped the spectra to contain a minimum of 25 photons per bin and rebinned the data to not to oversample the intrinsic energy resolution by a factor larger than 3.

2.2 *Swift* data

A total of four observations were obtained of IGR J17494–3030 with the XRT (Burrows et al. 2005) on board *Swift* (Gehrels et al. 2004). Three observations were performed in photon counting (PC) mode and one in windowed timing (WT) mode (Table 1). We processed the data making use of the HEASOFT v.6.12 software. The data reduction was carried out running the XRTPIPELINE task. For every observation, spectra, light curves and images were obtained using XSELECT. For the WT data, we used a circular region radius of ∼76 arcsec centred on the source position to extract the source events, and a similar region far enough from the source to extract the background events. For the PC data, we used a circular region of ∼47 arcsec centred on the source position to extract the source events and three circular regions of similar size for the background data. Observations 00032318001 and 00032318003 are affected by pile-up. To mitigate the pile-up effects, we excluded the inner ∼11 arcsec (observation 00032318001) and ∼9 arcsec (00032318003) from the central part of the source regions. We created exposure maps and ancillary response files following the standard *Swift* analysis threads, and we acquired the last version of the response matrix files from the HEASARC calibration data base (v.14). We grouped the spectra to have at least 20 counts per bin.

3 ANALYSIS AND RESULTS

3.1 Spectral analysis

We used XSPEC (v.12.8; Arnaud 1996) to fit the spectra. We incorporated in our models the photoelectric absorption component (PHABS) to account for the interstellar absorption. We simultaneously fitted the spectra obtained with the different *XMM–Newton*/EPIC detectors; the two MOS spectra were fitted in the energy range 0.5–10 keV and the PN spectrum in the 0.7–10 keV range. We tied all the parameters between the three detectors and introduced a constant factor (CONSTANT) to account for cross calibration uncertainties between the instruments. It was fixed to one for the PN spectrum and allowed to vary freely for the MOS ones. A single power-law (POWERLAW) model returns a hydrogen column density (N_H) of 1.87 × 10^{22} cm^{-2} and a power-law photon index (Γ) of 2.14. However, with a reduced $\chi^2(\chi^2_\nu)$ of 1.28 for 421 degrees of freedom (dof), the fit is not acceptable. Adding a soft blackbody component (BBODYRAD) to the power-law model improves the fit. The resulting spectra with the best-fitting model are shown in Fig. 1.

This two components model adequately fits the spectra ($\chi^2_\nu = 0.94$ for 419 dof), yielding $N_H = 1.8 \times 10^{22}$ cm^{-2}, $\Gamma = 1.76$ and $kT = 0.37$ keV (blackbody temperature). The inferred 0.5–10 keV unabsorbed flux is 1.13×10^{-11} erg cm^{-2} s^{-1}, of which ∼17 per cent is due to the thermal component. The full results of the fits are summarized in Table 2, in which the parameter errors are given with 90 per cent of confidence level and the flux errors were calculated as described by Wijnands et al. (2004). Although the source distance is unknown, the fact that the source position is close to the Galactic Centre ($l = 359.086$, $b = -01.511$), we assume a distance of 8 kpc for IGR J17494–3030 which is consistent with the relatively high N_H we obtained in the spectral fits.

The spectra were equally well fitted using neutron-star atmosphere models for the soft component. We used the NSATMOS model (Heinke et al. 2007). In this we assume that the accretor in the system is a neutron star but we note that the nature of the primary is still unknown. We fixed the mass of the putative neutron star to

[1] See table 3 in section 3.2.2 of the *XMM–Newton* Users Handbook: http://heasarc.gsfc.nasa.gov/docs/xmm/uhb/epicmode.html.
[2] See the calibration technical note XMM-SOC-CALTN-0083

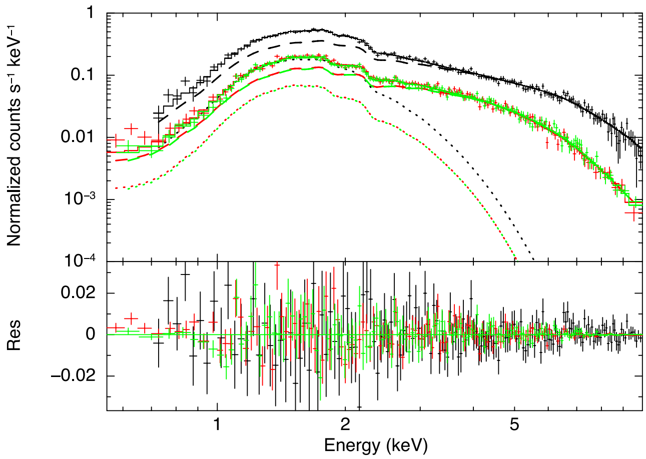

Figure 1. PN (black), MOS1 (red) and MOS2 (green) spectra of IGR J17494–3030. The solid line represented the best-fitting using a BBODYRAD+POWERLAW model. The dotted lines are the contribution of the thermal component and the dashed lines the contribution of the power law. The sub-panel shows the residuals.

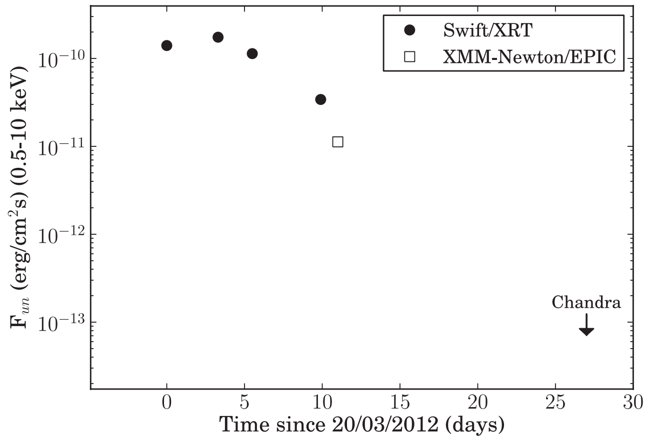

Figure 2. The unabsorbed flux (0.5–10 keV) evolution. Black circles represent the *Swift* observations while the white square represent the *XMM–Newton* one. The arrow is the upper limit calculated from the upper limit on the source count rate observed using *Chandra* (Chakrabarty et al. 2013).

1.4 $M_\odot$ and the radius to 10 km. We used a distance D of 8 kpc and we set the normalization to 1 (i.e. the whole surface is assumed to emit radiation), which leaves the neutron-star temperature as the only parameter free for the NSATMOS model. The obtained temperature (for an observer at infinity) is $kT^{\infty} = 0.182 \pm 0.004$ keV and the soft component contributes ~22 per cent to the total 0.5–10 keV unabsorbed flux. The other fit parameters are, within the errors, consistent with the values obtained when using the BBODYRAD model (see Table 2).

All *Swift* spectra are well described with a single absorbed power-law model (see Table 2). We fixed $N_{\rm H}$ to the value obtained from the *XMM–Newton* fit (1.87×10^{22} cm^{-2}). The photon index value is, within the errors, consistent in all observations. The peak unabsorbed flux is $\sim 1.7 \times 10^{-10}$ erg cm^{-2} s^{-1} (as observed during the second *Swift* observation) which corresponds to an $L_{\rm X}$ of $\sim 1.3 \times 10^{36} (D/8\,{\rm kpc})^2$ erg s^{-1} (0.5–10 keV). The lowest detected flux was observed during the *XMM–Newton* observation. The unabsorbed flux decreased approximately one order of magnitude in ~8 d (see also Fig. 2), which gives a luminosity seen during the *XMM–Newton* observation of $\sim 8.6 \times 10^{34} (D/8\,{\rm kpc})^2$ erg s^{-1}. We calculated the 0.5–10 keV unabsorbed flux upper limit from the *Chandra* count rate upper limit reported in Chakrabarty et al. (2013) using WebPIMMS. We assumed an absorbed power-law model with $N_{\rm H} = 1.87 \times 10^{22}$ cm^{-2} and $\Gamma = 2.14$ (the values obtained from the *XMM–Newton* spectra). The calculated 0.5–10 keV unabsorbed flux is $< 6.8 \times 10^{-14}$ erg cm^{-2} s^{-1} which results in a luminosity of $< 5.2 \times 10^{32} (D/8\,{\rm kpc})^2$ erg s^{-1} (see Fig. 2).

3.2 Light curve analysis

The count rate curve obtained during the *XMM–Newton* shows that the source intensity decreased during the observation, from ~0.65 to ~0.25 counts s^{-1} within ~12 h (see Fig. 2). In order to study the spectral evolution during the observation, we divided the observation in three segments of ~14.5 ks each and individually fitted each spectrum (both the PN and MOS spectra simultaneously). We used the absorbed NSATMOS + POWERLAW model with the $N_{\rm H}$ fixed to the value obtained from the fit using the data obtained from the whole observation (see Section 3.1). While the power-law index is constant within the errors ($\Gamma \sim 1.7$), the temperature decreases from $kT^{\infty} = 0.190 \pm 0.004$ to 0.170 ± 0.005 keV (Fig. 3; the errors are for 1σ). We can fit this decrease adequately with an exponential decay function with an e-folding time of $3.0^{+1.4}_{-0.7}$ d or with a power-law decay function with an index of –0.06 ± 0.02 (see

Table 2. Results from the spectral fits.

Instrument/ Obs ID	$N_{\rm H}$ (10^{22} cm^{-2})	Γ	kT (keV)	$T_{\rm fr}$ (per cent)	$F_{\rm X,\,abs}$ (10^{-11} erg cm^{-2} s^{-1})	$F_{\rm X,\,unabs}$	$L_{\rm X}$ (10^{35} erg s^{-1})	χ^2_ν (dof)
Swift/XRT				PHABS*(POWERLAW)				
00032318001	1.8 (fix)	1.8 ± 0.2	–	–	8.6 ± 0.7	14.0 ± 0.2	10.7 ± 0.8	0.99 (15)
00032318002	1.8 (fix)	1.9 ± 0.1	–	–	10.2 ± 0.4	17.4 ± 0.1	13.4 ± 0.8	0.98 (79)
00032318003	1.8 (fix)	1.8 ± 0.3	–	–	6.9 ± 0.9	11.3 ± 0.3	8.7 ± 0.8	0.53 (9)
00032318004	1.8 (fix)	2.0 ± 0.3	–	–	1.8 ± 0.2	3.4 ± 0.2	2.6 ± 0.8	0.92 (13)
XMM/EPIC				PHABS*(POWERLAW+BBODYRAD)				
0694040201	1.80 ± 0.07	1.76 ± 0.08	0.37 ± 0.03	17.3	0.649 ± 0.005	1.13 ± 0.05	0.86 ± 0.05	0.94 (419)
				PHABS*(POWERLAW+NSATMOS)				
	1.89 ± 0.03	1.74 ± 0.07	0.182 ± 0.004	22.9	0.649 ± 0.003	1.18 ± 0.01	0.90 ± 0.01	0.94 (420)

Note. Quoted errors represent 90 per cent confidence levels. The fifth column reflects the fractional contribution of the thermal component to the total unabsorbed 0.5–10 keV flux. $F_{\rm X,abs}$ and $F_{\rm X,unabs}$ represent the absorbed and unabsorbed fluxes (0.5–10 keV), respectively. The luminosity $L_{\rm X}$ (0.5–10 keV) was calculated adopting a distance of 8 kpc. The kT for the NSATMOS model is for an observer in infinity.

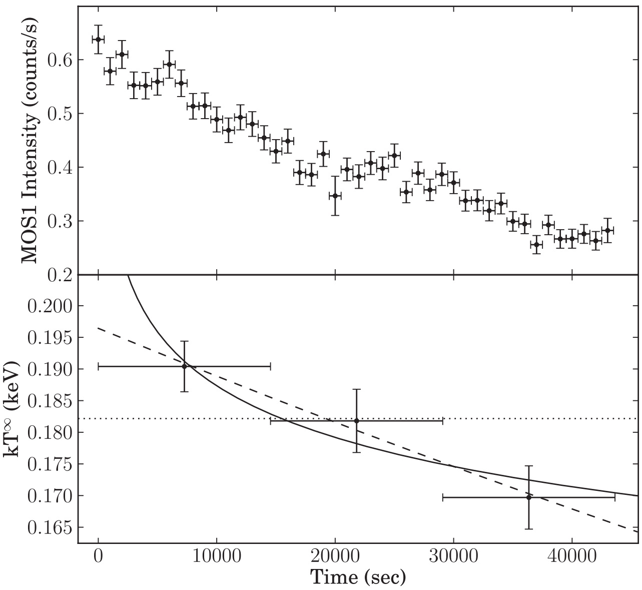

Figure 3. Upper panel: the MOS1 count rate curve using a bin size of 1000 s. Bottom panel: the evolution in the temperature during the *XMM–Newton* observation. The solid-line is the fit using a power-law decay model (with an index of -0.06 ± 0.02), the dashed line is the fit assuming an exponential decay function (with an *e*-folding time of ∼3 d) and the dotted line is the fit assuming a constant value (which does not provide an adequate fit).

Fig. 3).[3] We also tried a constant value, but that did not provide an adequate fit (with a χ^2 of 10.5 and a dof of 2, resulting in a *p*-value of 0.005). Both the flux observed from the soft component and the power-law component decrease during the observation. The thermal contribution to the 0.5–10 keV remained approximately constant during the decay.

4 DISCUSSION

We present the spectral analysis of the *Swift* and *XMM–Newton* observations of IGR J17494–3030 during its 2012 outburst. If we assume a distance of 8 kpc, the inferred peak luminosity is $L_X \sim 1.3 \times 10^{36}$ erg s^{-1} in the energy range 0.5–10 keV. However, the luminosity in the 2–10 keV energy range is only $L_X \sim 7.7 \times 10^{35}$ erg s^{-1}, making this source a very faint X-ray transient (Wijnands et al. 2006).

The intensity, amplitude, duration and X-ray spectral properties of the outburst of IGR J17494–3030 strongly suggest that this new X-ray transient is an LMXB. While the *Swift* spectra are well described by a simple absorbed power-law model with a photon index Γ of ∼2, the *XMM–Newton* spectra need an additional thermal component to be adequately modelled. This thermal component could possibly arise from an accretion disc (a disc blackbody model can adequately fitted the data), in which case we cannot determine whether the accreting object is a neutron star or a black hole. However, accretion discs at these low luminosities are typically expected to be at lower temperatures than what we observe, which suggests that the thermal component may have a different origin. In fact, the presence of the soft component (and its associated temperature) in the X-ray spectrum of IGR J17494–3030 is reminiscent of what is seen in neutron-star X-ray binaries at similar luminosities (e.g. Fridriksson et al. 2010; Armas Padilla et al. 2013b; Degenaar, Wijnands & Miller 2013). In those systems, the thermal component is thought to originate from the surface of the neutron star. Given the strong similarities, we tentatively identify the accretor in IGR J17494–3030 as a neutron star.

If the soft component is indeed originating from the neutron-star surface, then it is likely due to low-level accretion on to the surface. Such low-level accretion will indeed produce a soft spectrum (Zampieri et al. 1995) and in principle one should use the so-called Zamp model (Soria et al. 2011) to fit the soft component in the X-ray spectra. However, that model is not publicly available so the next best things are the neutron-star atmosphere models. Although those models assume that the emission is from a cooling neutron star and therefore incorporate different microphysics compare to the Zamp model, typically the results are very similar between the models (i.e. the inferred surface temperature; Soria et al. 2011). Therefore, we will discuss the results obtained using neutron-star atmosphere models which also allows for direct comparison with previous work in which only neutron-star atmosphere models were used.

During the *XMM–Newton* observation we see a steady decrease of the source intensity. Together with the intensity, the temperature of the soft component is decreasing as well. Although such a temperature decrease with decreasing intensity would be expected irrespectively if the soft component is due to a cooling accreting disc or due to decreasing accretion on to the neutron-star surface, it is very similar to what recently has been found for the bright neutron-star X-ray transient XTE J1709–267 by Degenaar et al. (2013). Those authors found that a similar (albeit at slightly lower luminosities and lower inferred surface temperatures) decay during the end stages of the 2012 outburst of XTE J1709–267. They favoured an interpretation that the observed temperature decrease was due to the cooling of the neutron-star crust which was heated by the accretion during the outburst.

However, the outburst of IGR J17494–3030 was much shorter (3–4 weeks versus 10 weeks) and much less luminous (peaking at $\sim 7 \times 10^{35}$ erg s^{-1} versus $\sim 5 \times 10^{37}$ erg s^{-1}; 2–10 keV) than that of XTE J1709–267. Within our understanding of crustal heating and cooling models, IGR J17494–3030 should have been heated to a much lesser extent (if at all). It would not be expected to display similarly strong signs of crustal cooling as XTE J1709–267. Therefore, this likely is not the correct interpretation of the observed rapid intensity decay during the *XMM–Newton* observation for IGR J17494–3030. Since the behaviour of this source is as similar as what has been observed for XTE J1709–267, likely also in that source we did not observe the crust cooling.

Degenaar et al. (2013) alternatively suggested that the temperature decrease observed for XTE J1709–267 was not due to a cooling crust but maybe the thermal component was due to low-level accretion on the neutron-star surface and the accretion rate decreased causing the surface temperature to decrease as well. This scenario could more naturally account for the similarities in the decay seen for the two sources, despite their different outburst properties. Therefore, we favour a low-level accretion scenario to explain the thermal component in both sources. If this is indeed the correct interpretation for the decay seen in both sources, then there is no need for an additional heat source in the neutron-star crust, as was proposed by Degenaar et al. (2013).

Moreover, investigating the literature for more detections of soft thermal components at such low-accretion luminosities of

[3] As reference time we used the start of the *XMM–Newton* observation, but we found that the *e*-folding time or index is not very sensitive to the exact value of the reference time.

accreting neutron-star systems (or candidate neutron-star systems), we find several additional sources which are consistent with the hypothesis that the soft thermal component in the luminosity range of 10^{34}–10^{35} erg s^{-1} is due to low-level accretion on to the neutron-star surface. For example, for the suspected neutron-star very faint X-ray transient XTE J1719–291 and for two confirmed persistent neutron-star VFXBs (1RXH J173523.7–354013, 1RXS J171824.2–402934), we found in previous work that their spectra also required a thermal component in addition to the power-law component (Armas Padilla et al. 2011; Armas Padilla et al. 2013b). We refitted their spectra with the NSATMOS model (we previously used black-body models) and obtained temperatures of 0.162 ± 0.004 keV, 0.184 ± 0.004 keV and 0.194 ± 0.003 keV, respectively, with associated luminosities of 3.3×10^{34}, 4.4×10^{34} and 6.7×10^{34} erg s^{-1}. In addition, Fridriksson et al. (2010) reported on a brief accretion flare during the quiescent state of the neutron-star X-ray transient XTE J1701–462 during which the temperature was 0.159 ± 0.02 keV for a luminosity of 2.6×10^{34} erg s^{-1}.

Uncertainties in the distances affect the inferred temperatures, but there appears to be a tendency that for higher luminosities, the temperature is higher, as one would expect for the low-level accretion scenario. This provides strong evidence that in all these sources the thermal component indeed arises from the neutron-star surface as a result of low-level accretion and that the inferred temperature is determined by the instantaneous mass accretion rate.

The decrease of surface temperature while the luminosity (and thus the inferred accretion rate on to the neutron-star surface) decreases can only continue (in the transient sources) as long as the temperature due to the low-level accretion is higher than the interior (crust) temperature of the neutron star. If the accretion rate drops below a certain value, then the light-curve evolution will not be governed anymore by the decay in accretion rate but instead it will be determined by how fast the crust cools down (even small outbursts will have a slightly heated crust) and eventually by the core cooling rate. Therefore, in the light curve we would expect a break at a certain luminosity from a rapid decay of the luminosity to a much slower decay rate. Such a break has been observed in several systems (e.g. XTE J1701–462 by Fridriksson et al. 2010; MAXI J0556–332 by Homan et al., in preparation; Aql X-1 by Campana et al. 1998; Campana et al., in preparation) and indeed has been interpreted as the onset of the crust cooling (e.g. Fridriksson et al. 2010).

ACKNOWLEDGEMENTS

We acknowledge the *XMM–Newton* team for make this observation possible. RW and MAP are supported by an ERC starting grant awarded to RW. ND is supported by a NASA Hubble Postdoctoral Fellowship grant (number HST-HF-51287.01-A) from the Space Telescope Science Institute.

REFERENCES

Armas Padilla M., Degenaar N., Patruno A., Russell D. M., Linares M., Maccarone T. J., Homan J., Wijnands R., 2011, MNRAS, 417, 659
Armas Padilla M., Degenaar N., Russell D. M. M., Wijnands R., 2013a, MNRAS, 428, 3083
Armas Padilla M., Degenaar N., Wijnands R., 2013b, MNRAS, 434, 1586
Arnaud K. A., 1996, in Jacoby G. H., Barnes J., eds, ASP Conf. Ser. Vol. 101, XSPEC: The First Ten Years. Astron. Soc. Pac., San Francisco, p. 17
Boissay R. et al., 2012, Astron. Telegram, 3984, 1
Bozzo E. et al., 2012, Astron. Telegram, 3989, 1
Burrows D. N. et al., 2005, Space Sci. Rev., 120, 165
Campana S., 2009, ApJ, 699, 1144
Campana S., Stella L., Mereghetti S., Colpi M., Tavani M., Ricci D., Dal Fiume D., Belloni T., 1998, ApJ, 499, L65
Chakrabarty D., Jonker P. G., Markwardt C. B., 2013, Astron. Telegram, 4886, 1
Degenaar N., Wijnands R., 2009, A&A, 495, 547
Degenaar N., Wijnands R., 2010, A&A, 524, A69
Degenaar N., Wijnands R., Miller J. M., 2013, ApJ, 767, L31
Fridriksson J. K. et al., 2010, ApJ, 714, 270
Gehrels N. et al., 2004, ApJ, 611, 1005
Heinke C. O., Jonker P. G., Wijnands R., Taam R. E., 2007, ApJ, 660, 1424
Jansen F. et al., 2001, A&A, 365, L1
Minniti D. et al., 2010, New Astron., 15, 433
Muno M. P., Pfahl E., Baganoff F. K., Brandt W. N., Ghez A., Lu J., Morris M. R., 2005, ApJ, 622, L113
Soria R., Zampieri L., Zane S., Wu K., 2011, MNRAS, 410, 1886
Strüder L. et al., 2001, A&A, 365, L18
Turner M. J. L. et al., 2001, A&A, 365, L27
Wijnands R., Homan J., Miller J. M., Lewin W. H. G., 2004, ApJ, 606, L61
Wijnands R. et al., 2006, A&A, 449, 1117
Zampieri L., Turolla R., Zane S., Treves A., 1995, ApJ, 439, 849

This paper has been typeset from a TEX/LATEX file prepared by the author.